

Journal of Materials Chemistry A

Accepted Manuscript



This is an *Accepted Manuscript*, which has been through the Royal Society of Chemistry peer review process and has been accepted for publication.

Accepted Manuscripts are published online shortly after acceptance, before technical editing, formatting and proof reading. Using this free service, authors can make their results available to the community, in citable form, before we publish the edited article. We will replace this *Accepted Manuscript* with the edited and formatted *Advance Article* as soon as it is available.

You can find more information about *Accepted Manuscripts* in the [Information for Authors](#).

Please note that technical editing may introduce minor changes to the text and/or graphics, which may alter content. The journal's standard [Terms & Conditions](#) and the [Ethical guidelines](#) still apply. In no event shall the Royal Society of Chemistry be held responsible for any errors or omissions in this *Accepted Manuscript* or any consequences arising from the use of any information it contains.

ARTICLE

Self-assembly of Polyoxometalates, Pt Nanoparticles and Metal-Organic Frameworks into a Hybrid material for Synergistic Hydrogen Evolution

Cite this: DOI: 10.1039/x0xx00000x

Received 00th January 2012,
Accepted 00th January 2012

DOI: 10.1039/x0xx00000x

www.rsc.org/

Weiwei Guo, Hongjin Lv, Zheyuan Chen, Kevin P. Sullivan, Sarah M. Lauinger, Yingnan Chi, Jordan M. Sumliner, Tianquan Lian and Craig L. Hill*

A polyoxometalate (POM), Pt nanoparticles (NPs) and a metal-organic framework (MOF, NH₂-MIL-53) self-assemble into a hybrid material, **PNPMOF**, that displays synergistic activity for visible-light-driven catalytic hydrogen evolution (the **PNPMOF** is far more active than any of the three functional components alone). The POM has four targeted functions in this hybrid material: it reduces H₂PtCl₆ to Pt NPs, stabilizes the Pt NPs, induces a strong electrostatic association of the negatively charged Pt NPs with the protonated NH₂-MIL-53 sites on the particle surfaces, and facilitates the catalytic reduction reaction itself. The NH₂-MIL-53 in this work protects the light sensitive 2-aminoterephthalate groups in the pores from oxidation by the POMs, while the surface protonated NH₂ units on the MOF particle surfaces strongly bind the negatively-charged POM-stabilized Pt NPs.

Introduction

Developing artificial photosynthetic systems that harvest sunlight, the most abundant source of renewable energy, has become a major goal of the research community.¹⁻⁸ Two essential components are needed for a light-driven photosynthetic system: the photosensitizer for light harvesting and the catalyst for water splitting and/or for carbon dioxide fixation.⁹ Recent progress has been made on various fronts lately including the use of semiconductors,¹⁰ metalloporphyrins,^{11, 12} polyoxometalates (POMs)¹³⁻²⁰ and metal-organic frameworks (MOFs)²¹⁻²⁶ as potential catalysts. POMs, a family of metal oxide cluster polyanions with highly variable functional properties, have applications in molecular magnetism, medicine and catalysis.²⁷⁻³⁶ Some POM catalysis is facilitated by their rich, and reversible redox chemistry.³⁷⁻³⁹ POMs stabilize noble-metal nanoparticles (NPs).⁴⁰⁻⁴³ The stabilized Pt NPs show enhanced activities in multiple reactions relative to commercial Pt black.^{44, 45} For example, CdS quantum dots with POM-encapsulated gold NPs are more efficient photocatalysts for H₂ evolution than gold NPs without POMs.⁴⁶

Simultaneously, noteworthy studies on photoactive MOF-based catalysis for energy-related reactions including water splitting and CO₂ reduction have gained much attention.^{21-23, 47-51} MOFs are a class of crystalline porous functional materials constructed from metal-oxide unites and organic linkers. The ultrahigh porosity and

high thermal stability together with the potential active sites for redox reactions have led to some successful applications of MOFs in various fields: gas storage and separation, nonlinear optics and catalysis.⁵²⁻⁵⁶ For example, Lin and co-workers utilized a mix-and-match strategy to synthesize a series of photoactive MOFs for visible-light-driven CO₂ reduction and water splitting.^{47, 48, 57}

MOF composites have also been well-documented.⁵⁸ MOFs containing POMs and/or metal NPs have shown synergistic activity.⁵⁹⁻⁶⁷ Our group previously reported a Cu-containing POM-MOF that catalyzes aerobic sulfoxidation in which the MOF and the encapsulated POM exhibit synergistic hydrolytic stability and catalytic activity.⁶² MOFs are well documented to encapsulate NPs.⁶⁸ For example, MIL-101 with encapsulated gold NPs shows synergistic aerobic alcohol oxidation.⁶³

We report here an approach that combines POMs, Pt NPs and MOFs in a hybrid material, POM-Pt NPs@NH₂-MIL-53 (**PNPMOF**), with greatly enhanced photocatalytic H₂ evolution relative to each component alone. Pt NPs which are stabilized by Keggin POMs (H₃PW₁₂O₄₀) are loaded onto the surfaces of amine-functionalized MOF, NH₂-MIL-53 particles. This work also demonstrates that a POM can perform four separate functions simultaneously, a theme of potential value in construction of energy converting multicomponent assemblies. The stability of the **PNPMOF** composite under catalytic conditions was also investigated.

Experimental Section

General Methods and Materials

All chemicals used were from commercially available sources and were used without further purification unless otherwise noted. Infrared spectra (2% sample in KBr pellet) were recorded on a Nicolet TM 600 FT-IR spectrometer. Thermogravimetric analyses were performed on a STA 6000 thermal analyzer. Surface area measurement was carried out on a NOVA 200 BET surface analyzer from Quantachrome Corporation. Transmission electron microscopy (TEM) and Z-contrast TEM (Z-TEM) images were taken on a Hitachi H-7500 transmission electron microscope at an accelerating voltage of 75 kV. Scanning Electron Microscopy (SEM) images were obtained on a High Resolution S4800 Scanning Electron Microscope operated at 30 kV. Energy-dispersive X-ray (EDX) analysis was performed on this SEM coupled with an EDX Si(Li) X-ray detector. The samples for TEM and SEM were prepared by dropping and coating the sonicated aqueous sample solution onto a carbon-coated copper grid and air dried. Steady-state luminescence quenching spectra were obtained using a FluoroMax 3 spectrofluorimeter. Time-resolved fluorescence decay measurements were conducted using a mode-locked Ti:sapphire laser (Tsunami oscillator pumped by 10 W Millennia EV, Spectra-Physics). Excitation pulses at 400 nm were generated by the second harmonic generation of the 800 nm pulses in a BBO crystal. The 540-620 nm emissions were detected using a microchannel plate photomultiplier tube (Hamamatsu R3809U-51). The repetition rate of output pulses centered at 800 nm was reduced from 80 MHz to 9MHz by a pulse picker (Conoptics, USA). The output was amplified and analyzed using a TCSPC board (Becker & Hickel SPC 600). UV-vis spectra were obtained on an Agilent 8453 spectrophotometer equipped with a diode-array detector using a 1.0-cm-optical-path quartz cuvette. Visible diffuse reflectance spectra were obtained using Miniscan XE Plus from Hunter Associates Lab. Elemental analyses (Al, P, W, Pt and N) were performed by Galbraith Laboratories (Knoxville, Tennessee). The Powder XRD data were collected on a D8 Discover Powder Instrument on monochromatic Cu K α ($\gamma = 1.54060$ Å) radiation. Amounts of hydrogen in the photocatalytic reduction experiments were measured by gas chromatography (GC) using a 5 Å molecular sieve column and a TCD detector with Ar as the carrier gas.

Syntheses

Synthesis of NH₂-MIL-53. The NH₂-MIL-53 was prepared by a modified literature method.⁶⁹ Typically, 0.153 g of aluminum chloride hexahydrate (0.63 mmol) was mixed with 0.168 g 2-aminoterephthalic acid (0.93 mmol) in 9 mL DMF. The solution was kept at 150 °C in a Teflon-lined autoclave bomb. After 72 h, the solids were separated by centrifugation and washed with DMF three times and with methanol three times. The solids were then dried under vacuum at 80 °C for 6 h. Yield: 0.05 g, 38%.

Synthesis of POM-Pt NPs@NH₂-MIL-53 (PNPMOF). Isopropanol (14 μ L) and H₂PtCl₆ (10 μ L of 0.5 M) were added to an aqueous solution of 2 mL of H₃PW₁₂O₄₀ (0.1 M). The mixture was irradiated using a UV lamp for 2 h, and the color of the solution changed from light yellow to dark blue. The dark-blue solution was then mixed with 50 mg NH₂-MIL-53 and exposed to air forming **PNPMOF**. This product composite was separated by centrifugation and washed extensively with methanol and water.

Synthesis of POM-Pt NPs@NH₂-silica. This hybrid was prepared using a procedure similar to that used for **PNPMOF** except that commercial amino-functionalized silica gel was used instead of NH₂-MIL-53.

Photocatalytic experimental processes

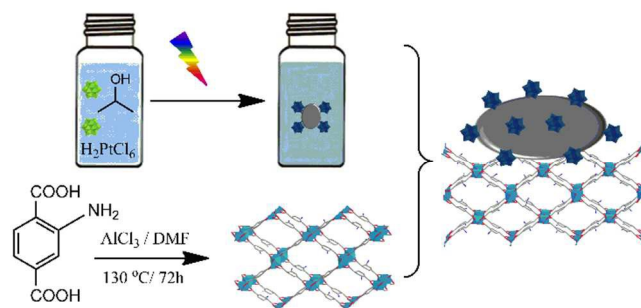
The hydrogen evolution experiments were conducted in 2.5 mL septum-sealed glass vials containing 10 mg of **PNPMOF**. Typically, 2 mL of aqueous ascorbic acid (0.05-0.2 M) and 10 mg **PNPMOF** were added to the vials. The pH of the solution was adjusted by adding 0.1 M NaOH before use. The vials were then capped and deoxygenated by bubbling Ar for 30 min and irradiated by a Xe-lamp source (light intensity 150W, beam size 0.2 cm², 400 nm cutoff filter) at room temperature and magnetically stirred for 6 h. The hydrogen in the headspace of the vials was analyzed by GC.

Recycle and Reuse

The solid in the reaction mixture after each photocatalytic experimental entry was collected by centrifugation and washed repeatedly with distilled water. The filtrate solution was investigated by UV-vis spectroscopy and analyzed by elemental analysis to detect any leaching of organic ligands or Pt NPs. The solid was then dried under vacuum before being used in successive catalytic runs. All reactions were conducted under the same conditions.

Results and Discussion

Scheme 1 illustrates the preparation for **PNPMOF**. The POM-stabilized Pt NPs were prepared following a modified literature method.⁴⁴ H₃PW₁₂O₄₀ was first reduced by isopropanol upon UV light irradiation, and the dark blue reduced [PW₁₂O₄₀]⁴⁻ product then was used to reduce H₂PtCl₆ forming Pt NPs. The negatively-charged POMs are well known to attach to the surface of Pt NPs and to stabilize these against aggregation.⁴⁰⁻⁴³ The resulting POM-stabilized Pt NPs were mixed with the amine-functionalized MOF, NH₂-MIL-53 which was prepared following a modified literature method,⁶⁹ forming **PNPMOF**. **PNPMOF** is partly cationic, i.e. bearing NH₃⁺ groups below pH ~6 which electrostatically bind the negatively charged POM-stabilized Pt NPs. The final **PNPMOF** contains H₃PW₁₂O₄₀ and Pt NPs in 3.92 and 0.38 weight percents respectively by elemental analysis.



Scheme 1. Route to **PNPMOF** (symbols not to scale). Green polyhedra: H₃PW₁₂O₄₀; dark blue polyhedra: reduced POM units, [PW₁₂O₄₀]⁴⁻; gray ellipsoids: Pt NPs; light blue octahedra: AlO₄(OH)₂; gray sticks: carbon connector units; dark blue sticks: -NH₂ side chains; red sticks: oxygen.

The **PNPMOF** shows a PXRD pattern and an FT-IR spectrum that are very similar to those of $\text{NH}_2\text{-MIL-53}$ indicating that $\text{NH}_2\text{-MIL-53}$ structure is maintained (Figs 1A, 1B and S1). $\text{NH}_2\text{-MIL-53}$ is constructed by one-dimensional aluminum oxide chains joined together by 2-aminoterephthalate linkers.⁷⁰ The FT-IR spectrum (Fig 1B) of **PNPMOF** shows typical bands of $\text{NH}_2\text{-MIL-53}$. The characteristic bands attributed to the symmetric and asymmetric stretches of free NH_2 groups (3390 and 3501 cm^{-1}) confirms that the NH_2 groups are successfully incorporated into the framework.²² Moreover, the splitting of the band at *ca.* 1430 cm^{-1} corresponding to the symmetric stretches of carboxylate groups is introduced by the amino groups which lower the overall symmetry.⁷¹ However, the vibrational peaks for $\text{H}_3\text{PW}_{12}\text{O}_{40}$ are not easily distinguished because they overlap with the strong stretching peaks of the organic linkers in $\text{NH}_2\text{-MIL-53}$ at the low POM loading in **PNPMOF**. Nevertheless, the TEM images (Fig S2A and S2C) of **PNPMOF** show 50-80 nm Pt NPs are firmly adhering to the $\text{NH}_2\text{-MIL-53}$ particles. In contrast, the Z-TEM image of $\text{NH}_2\text{-MIL-53}$ mixed with the commercial Pt black (Fig S2D) shows that the Pt particles are heavily aggregated, and the Pt particles are not firmly binding to $\text{NH}_2\text{-MIL-53}$ surfaces. This indicates that the POMs binding to the surface of the Pt(0) NPs greatly inhibit NP aggregation. We calculate that *ca.* 6% of the total NH_2 groups in the entire MOF sample are connected to the Pt NPs on the particle surfaces (see Scheme S1 in SI for detailed calculations). EDX spectroscopy further confirms the existence of the POM-stabilized Pt NPs as well as the $\text{NH}_2\text{-MIL-53}$ particles: distinct peaks for W and Pt are seen (Fig S3). The **PNPMOF** has a similar thermal behavior to $\text{NH}_2\text{-MIL-53}$ (Fig S4). The BET surface area of **PNPMOF** ($684\text{ m}^2/\text{g}$) is lower than that of $\text{NH}_2\text{-MIL-53}$ ($912\text{ m}^2/\text{g}$) (Fig S5-S7). These BET surface areas of 912 and $1174\text{ m}^2/\text{g}$ are consistent with previously reported literature values.⁶⁹

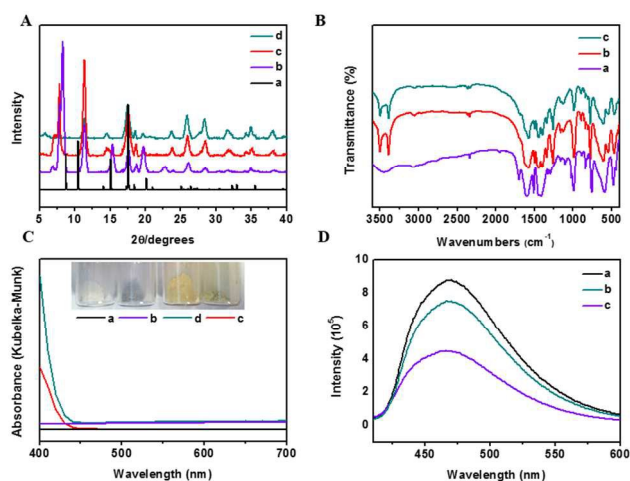


Fig 1. A) PXRD patterns of a) simulated MIL-53, b) MIL-53, c) $\text{NH}_2\text{-MIL-53}$ and d) **PNPMOF**. B) FT-IR spectra of a) MIL-53, b) $\text{NH}_2\text{-MIL-53}$ and c) **PNPMOF**. C) Diffuse reflectance spectra of a) MIL-53, b) POM-Pt NPs@MIL-53 (the MOF without the anilinium side chain), c) **PNPMOF** and d) $\text{NH}_2\text{-MIL-53}$. Inset: photograph of these samples in small vials. D) Photo-luminescence spectra of a) $\text{NH}_2\text{-MIL-53}$, b) $\text{NH}_2\text{-MIL-53}$ combined with $\text{H}_3\text{PW}_{12}\text{O}_{40}$ and c) **PNPMOF**. The weighed quantities of the MOF samples are the same in all spectra (Figs C and D).

Modification of the benzene-1,4-dicarboxylate organic linkers in MIL-125(Ti), with amino groups makes these units capable of absorbing visible light and transferring electrons to thermodynamically appropriate donors.²² Similarly, $\text{NH}_2\text{-MIL-53}$ exhibits a lone pair $n\text{-}\pi^*$ transition of the amino groups with an

absorption edge extending to 450 nm ,^{72, 73} consistent with its light yellow color (Fig 1C). As a result, $\text{NH}_2\text{-MIL-53}$ can function as robust light absorber in light-driven photocatalytic systems. The optical properties of **PNPMOF** are similar to those of $\text{NH}_2\text{-MIL-53}$. The presence of Pt NPs decreases the light harvesting ability of **PNPMOF**. The photo-luminescence spectra of **PNPMOF** are shown in Fig 1D. $\text{NH}_2\text{-MIL-53}$ displays a broad photo-luminescence with an emission maximum at 470 nm upon excitation at 400 nm , consistent with the known photo-luminescence of 2-aminoterephthalic acid.⁷⁴ When $\text{NH}_2\text{-MIL-53}$ is combined with $\text{H}_3\text{PW}_{12}\text{O}_{40}$, the emission intensity decreases, consistent with electron transfer between $\text{NH}_2\text{-MIL-53}$ and the POMs. In particular, a maximum decrease of intensity is observed in **PNPMOF**, which implies that electron transfer between $\text{NH}_2\text{-MIL-53}$ and the POM-stabilized Pt NPs is more efficient when $\text{NH}_2\text{-MIL-53}$, POMs and Pt NPs are all present but not bonded to one another. This is borne out by the synergistic catalytic activity of **PNPMOF**.

The **PNPMOF** was investigated for its photocatalytic H_2 evolution activity using ascorbic acid (AA) as sacrificial electron donor under visible light irradiation. The catalytic activity depends on solution pH (Fig 2A and S8). It maximizes at pH 4.5, at which point, the AA not only acts as a sacrificial reducing agent but also functions as a buffer with its reduced product, dehydroascorbic acid (dHAA).⁷⁵ At pH 4.5, *ca.* 1% of the NH_2 groups are protonated which can firmly bind the negatively charged Pt NPs; the remaining 99% that are unprotonated and can function as light absorbers (Fig S8).⁷⁶ Moreover, the activity increases slightly with AA concentration (Fig S9). In the following photocatalytic reactions, 0.1 M AA at pH 4.5 was used and is denoted as the standard conditions.

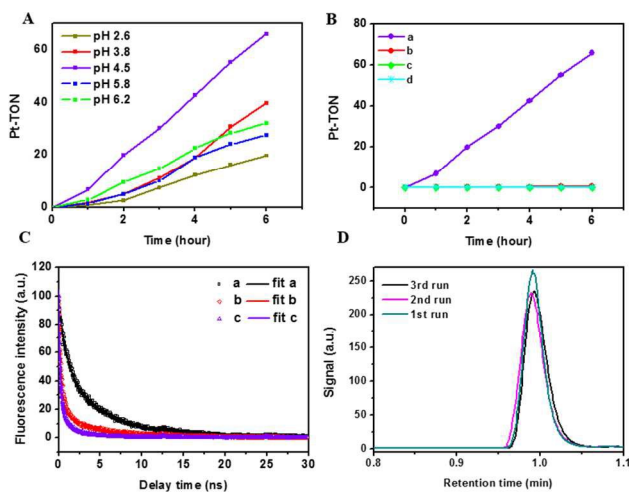


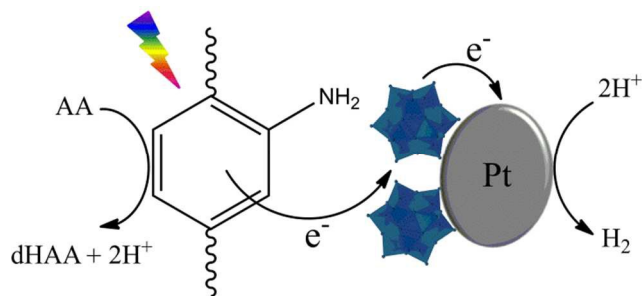
Fig 2. A) Time-dependent hydrogen evolution by **PNPMOF** under different pH conditions. B) Time-dependent H_2 evolution of a) **PNPMOF**, b) 2-aminoterephthalic acid mixed with POM-stabilized Pt NPs, c) $\text{NH}_2\text{-MIL-53}$ mixed with commercial Pt black and d) POM-Pt NPs@ $\text{NH}_2\text{-silica}$. "Pt-TON" are turnovers with respect to total Pt atoms. C) Normalized fluorescence decay of a) 2-aminoterephthalic acid in the solid state, b) $\text{NH}_2\text{-MIL-53}$, c) **PNPMOF**. The solid lines are best fits according to single exponential decay for a) and bi-exponential decays for b) and c). D) The hydrogen peak in GC traces in successive experiments using the same catalyst. (Fresh solutions were used for each run; reaction time = 6 h all cases).

A TON of *ca.* 66 is achieved in 6 hours under standard conditions (Fig 2B) with a quantum yield of 1.2×10^{-4} . In dramatic contrast, when POM-Pt NPs@ $\text{NH}_2\text{-silica}$ was used for photocatalytic H_2

production, no H₂ was detected because of the lack of a light absorbing unit. Significantly, the control experiment using commercial 2-aminoterephthalic acid instead of NH₂-MIL-53 only shows a TON of *ca.* 1 after 6 hours, which was presumably due to the fact that 2-aminoterephthalic acid was easily oxidized by POMs⁷⁷ thus losing its light absorbing ability (Fig S10). Moreover, this further indicates that the partially cationic NH₂-MIL-53 not only electrostatically binds to the negatively-charged Pt NPs but also helps to stabilize the 2-aminoterephthalic connectors. A similar stabilization effect of MOFs was observed previously.⁴⁷ In addition, it has been reported that the size of Pt NPs can affect the activity towards various reactions,⁷⁸⁻⁸² thus the efficiency of the photocatalytic system in this study might be further optimized via modifying the size of Pt NPs.⁶⁸

Importantly, a negligible amount of H₂ was identified when Pt black@NH₂-MIL-53 was used (Fig 2B), implying the importance of the POMs in catalytic turnover, and specifically in charge separation and electron transfer processes.⁸³⁻⁸⁵ The control experiments based on each component were conducted (Table S1). No obvious activity is observed for each component alone: the MOF, the POM, the Pt NPs and the AA are all essential for H₂ evolution, as is visible light (no H₂ is detected in the dark). In addition, the photocatalytic system is not temperature dependent: reactions in 0 °C, 25 °C and 50 °C water bath show almost identical activity (Table S1).

Fluorescence lifetime measurements were used to track the dynamics of photoexcited electrons in NH₂-MIL-53. As shown in Fig 2C, the excited state of 2-aminoterephthalic acid in the solid state decays single-exponentially with a lifetime of 3.0 ns, while the excited state of NH₂-MIL-53, shows a bi-exponential decay with an average lifetime of $\tau = (A_1\tau_1^2 + A_2\tau_2^2)/(A_1\tau_1 + A_2\tau_2) = 2.1$ ns. However, when the NH₂-MIL-53 is combined with POM-stabilized Pt NPs, the average lifetime is only 0.7 ns (Table S2). The decreased lifetime from 2.1 ns to 0.7 ns suggests that additional decay channels exist in the presence of POM-stabilized Pt NPs, such as electron transfer and energy transfer from the photoexcited NH₂-MIL-53. The H₂ evolution in the photoexcited **PNPMOF** indicates the existence of photo-induced electron transfer. As a negligible amount of H₂ is evolved in the absence of NH₂-MIL-53 (See Table S1), the photo-generated electrons have to be transferred from the photo-excited NH₂-MIL-53 to the POM-stabilized Pt NPs. Therefore, part of the decreased fluorescence lifetime is due to this electron transfer.



Scheme 2. Scheme showing the proposed mechanism for photocatalytic H₂ evolution in the **PNPMOF** system (symbols are not to scale)

Based on the above observations, a systematic mechanism for this light-induced H₂ evolution using **PNPMOF** as the catalyst and AA as the sacrificial electron donor is proposed in Scheme 2. Under visible light irradiation, the NH₂-MIL-53 forms electron-hole pairs. The electrons transfer to the POMs and then to the Pt NPs where H₂ is evolved.

The ATR-IR spectra indicate that this multi-component self-assembled photocatalyst system is quite stable from pH 2 to pH 8

(Fig S11). Moreover, the catalyst can be easily recycled and reused. After the first run, the catalyst was separated by centrifugation, washed with distilled water extensively and dried under vacuum. This recycled catalyst was reused for the second run. As shown in Fig 2D, the catalyst showed an activity comparable to that in the first run. In addition, the filtrate solution after the first run was examined by elemental analysis, and only a trace amount of H₃PW₁₂O₄₀ was detected indicating that no apparent H₃PW₁₂O₄₀ or Pt was leached into the solution under turnover conditions. No photocatalytic activity was detected using the filtrate solution. The UV-vis spectra of the solution after the first run indicated a negligible amount of organic linker was present arguing strongly that the MOF structure is maintained during the catalytic reactions (Fig S12). In addition, both the PXRD patterns and the FT-IR spectra of **PNPMOF** after catalysts retain all the characteristic peaks in the before-catalysis samples (Fig S13 and S14). The above observations confirm the robust nature of the **PNPMOF** composite.

Conclusions

In conclusion, POM-stabilized Pt NPs bind to NH₂-MIL-53 particles forming the **PNPMOF** which exhibits synergistic photocatalytic H₂ evolution activity (all 3 components alone are far less active). The surface protonated NH₂ units on the MOF particles bind the negatively-charged POM-stabilized Pt NPs, and the NH₂-MIL-53 in this work protects the light sensitive 2-aminoterephthalate groups from oxidation by the POMs as well. Significantly, the POMs exhibit four roles in the **PNPMOF**: they reduce H₂PtCl₆ to Pt NPs, stabilize Pt NPs, facilitate Pt NP association with the cationic support, and speed up catalytic H₂ evolution by promoting electron transfer between NH₂-MIL-53 and the catalytic Pt NPs. The **PNPMOF** composite is quite stable under turnover conditions. This work illustrates the prospect of other materials in which POMs exhibit more than one function including catalytic activity.

Acknowledgements

This work was supported by the U.S. Department of Energy, Office of Basic Energy Sciences, Solar Photochemistry Program, grant number DE-FG02-07ER15906. We thank Dr. John Bacsá for the X-ray powder diffraction analysis, Emory University Apkarian Integrated Electron Microscopy Core for electron microscopy, Hong Yi for the microscopy data, and Stefan Lutz for use of the spectrofluorimeter.

Notes and references

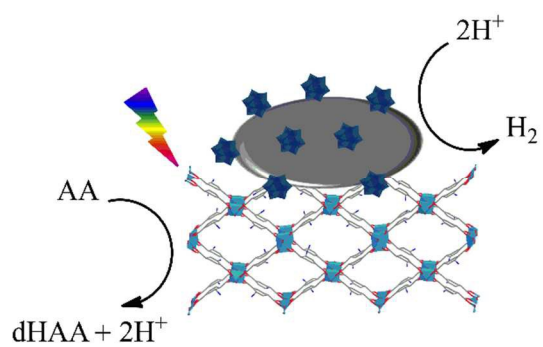
* Department of Chemistry, Emory University, 1515 Dickey Dr., Atlanta, Georgia 30322, USA
Email: chill@emory.edu

† Electronic Supplementary Information (ESI) available: [Details of synthesis, characterization and other catalytic results.]. See DOI: 10.1039/b000000x/

1. M. R. Wasielewski, *Acc. Chem. Res.*, 2009, **42**, 1910.
2. T. Faunce, S. Stryring, M. R. Wasielewski, G. W. Brudvig, A. W. Rutherford, J. Messinger, A. F. Lee, C. L. Hill, H. deGroot, M. Fontecave, D. R. MacFarlane, B. Hankamer, D. G. Nocera, D. M. Tiede, H. Dau, W. Hillier, L. Wang and R. Amal, *Energy Environ. Sci.*, 2013, **6**, 1074.
3. D. G. Nocera, *Acc. Chem. Res.*, 2012, **45**, 767.
4. T. Meyer, *Acc. Chem. Res.*, 1989, **22**, 163.
5. D. Gust, T. A. Moore and A. L. Moore, *Acc. Chem. Res.*, 2009, **42**, 1890.

6. P. D. Frischmann, K. Mahata and F. Würthner, *Chem. Soc. Rev.*, 2013, **42**, 1847.
7. A. J. Bard and M. A. Fox, *Acc. Chem. Res.*, 1995, **28**, 141.
8. J. J. Concepcion, R. L. House, J. M. Papanikolas and T. J. Meyer, *Proc. Natl. Acad. Sci.*, 2012, **109**, 15560.
9. Q. Yin, J. M. Tan, C. Besson, Y. V. Geletii, D. G. Musaev, A. E. Kuznetsov, Z. Luo, K. I. Hardcastle and C. L. Hill, *Science*, 2010, **328**, 342.
10. S. Hu, M. R. Shaner, J. A. Beardslee, M. Lichterman, B. S. Brunshwig and N. S. Lewis, *Science*, 2014, **344**, 1005.
11. M. K. Panda, K. Ladomenou and A. G. Coutsolelos, *Coord. Chem. Rev.*, 2012, **256**, 2601.
12. L.-L. Li and E. W.-G. Diau, *Chem. Soc. Rev.*, 2013, **42**, 291.
13. H. Lv, Y. V. Geletii, C. Zhao, J. W. Vickers, G. Zhu, Z. Luo, J. Song, T. Lian, D. G. Musaev and C. L. Hill, *Chem. Soc. Rev.*, 2012, **41**, 7572.
14. A. Dolbecq, E. Dumas, C. R. Mayer and P. Mialane, *Chem. Rev.*, 2010, **110**, 6009.
15. B. Rausch, M. D. Symes, G. Chisholm and L. Cronin, *Science*, 2014, **345**, 1326.
16. B. Matt, J. Fize, J. Moussa, H. Amouri, A. Pereira, V. Artero, G. Izzet and A. Proust, *Energy Environ. Sci.*, 2013, **6**, 1504.
17. H. Lv, J. Song, H. Zhu, Y. V. Geletii, J. Bacsa, C. Zhao, T. Lian, D. G. Musaev and C. L. Hill, *J. Catal.*, 2013, **307**, 48.
18. H. Fu, C. Qin, Y. Lu, Z.-M. Zhang, Y.-G. Li, Z.-M. Su, W.-L. Li and E.-B. Wang, *Angew. Chem. Int. Ed.*, 2012, **51**, 7985.
19. H. Lv, W. Guo, K. Wu, Z. Chen, J. Bacsa, D. G. Musaev, Y. V. Geletii, S. M. Lauinger, T. Lian and C. L. Hill, *J. Am. Chem. Soc.*, 2014, **136**, 14015.
20. Y. V. Geletii, Q. Yin, Y. Hou, Z. Huang, H. Ma, J. Song, C. Besson, Z. Luo, R. Cao, K. P. O'Halloran, G. Zhu, C. Zhao, J. W. Vickers, Y. Ding, S. Mohebbi, A. E. Kuznetsov, D. G. Musaev, T. Lian and C. L. Hill, *Isr. J. Chem.*, 2011, **51**, 238.
21. A. Fateeva, P. A. Chater, C. P. Ireland, A. A. Tahir, Y. Z. Khimyak, P. V. Wiper, J. R. Darwent and M. J. Rosseinsky, *Angew. Chem. Int. Ed.*, 2012, **51**, 7440.
22. Y. Fu, D. Sun, Y. Chen, R. Huang, Z. Ding, X. Fu and Z. Li, *Angew. Chem. Int. Ed.*, 2012, **51**, 3364.
23. J.-L. Wang, C. Wang and W. Lin, *ACS Catal.*, 2012, **2**, 2630.
24. F. X. L. i. Xamena, A. Corma and H. Garcia, *J. Phys. Chem.*, 2007, **111**, 80.
25. A. Corma, H. Garcia and F. X. Llabrés i Xamena, *Chem. Rev.*, 2010, **110**, 4606.
26. J. Gascon, A. Corma, F. Kapteijn and F. X. Llabrés i Xamena, *ACS Catal.*, 2013, **4**, 361.
27. M. T. Pope and A. Müller, *Angew. Chem.*, 1991, **103**, 56.
28. M. Sadakane, M. H. Dickman and M. T. Pope, *Inorg. Chem.*, 2001, **40**, 2715.
29. A. Proust, R. Thouvenot and P. Gouzerh, *Chem. Commun.*, 2008, 1837.
30. R. Neumann and A. M. Khenkin, *Chem. Commun.*, 2006, 2529.
31. J. T. Rhule, C. L. Hill, D. A. Judd and R. F. Schinazi, *Chem. Rev.*, 1998, **98**, 327.
32. W. Guo, Z. Luo, H. Lv and C. L. Hill, *ACS Catal.*, 2014, **4**, 1151.
33. R. N. Biboum, C. P. N. Njiki, G. Zhang, U. Kortz, P. Mialane, A. Dolbecq, I. M. Mbomekalle, L. Nadjjo and B. Keita, *J. Mater. Chem.*, 2011, **21**, 645.
34. H. N. Miras, J. Yan, D.-L. Long and L. Cronin, *Chem. Soc. Rev.*, 2012, **41**, 7403.
35. L. Cronin and A. Muller, *Chem. Soc. Rev.*, 2012, **41**, 7333.
36. H. N. Miras, G. J. T. Cooper, D.-L. Long, H. Bögge, A. Müller, C. Streb and L. Cronin, *Science*, 2010, **327**, 72.
37. C. L. Hill, *Nature*, 1999, **401**, 436.
38. C. L. Hill, ed., *Special Thematic Issue on Polyoxometalates*, 1998.
39. C. L. Hill, *Chem. Rev.*, 1998, **98**, 1.
40. J. D. Aiken, III and R. G. Finke, *J. Am. Chem. Soc.*, 1999, **121**, 8803.
41. S. Oezkar and R. G. Finke, *J. Am. Chem. Soc.*, 2002, **124**, 5796.
42. R. G. Finke, in *Metal Nanoparticles*, eds. D. L. Feldheim and C. A. Foss, Jr., Marcel Dekker, Inc., New York, N. Y., 2002, pp. 17.
43. Y. Wang and I. A. Weinstock, *Chem. Soc. Rev.*, 2012, **41**, 7479.
44. S. Mandal, P. Selvakannan, R. Pasricha and M. Sastry, *J. Am. Chem. Soc.*, 2003, **125**, 8440.
45. T. Hsu-Yao, K. P. Browne, N. Honesty and Y. J. Tong, *Phys. Chem. Chem. Phys.*, 2011, **13**, 7433.
46. X. Xing, R. Liu, X. Yu, G. Zhang, H. Cao, J. Yao, B. Ren, Z. Jiang and H. Zhao, *J. Mater. Chem. A*, 2013, **1**, 1488.
47. C. Wang, Z. Xie, K. E. deKrafft and W. Lin, *J. Am. Chem. Soc.*, 2011, **133**, 13445.
48. C. Wang, K. E. deKrafft and W. Lin, *J. Am. Chem. Soc.*, 2012, **134**, 7211.
49. D. Sun, Y. Fu, W. Liu, L. Ye, D. Wang, L. Yang, X. Fu and Z. Li, *Chem. Eur. J.*, 2013, **19**, 14279.
50. T. Zhou, Y. Du, A. Borgna, J. Hong, Y. Wang, J. Han, W. Zhang and R. Xu, *Energy Environ. Sci.*, 2013, **6**, 3229.
51. B. Nohra, H. El Moll, L. M. Rodriguez-Albelo, P. Mialane, J. é. Marrot, C. Mellot-Draznieks, M. O'Keeffe, R. Ngo Biboum, J. Lemaire, B. Keita, L. Nadjjo and A. Dolbecq, *J. Am. Chem. Soc.*, 2011, **133**, 13363.
52. M. Eddaoudi, J. Kim, N. Rosi, D. Vodak, J. Wachter, M. O'Keeffe and O. M. Yaghi, *Science*, 2002, **295**, 469.
53. O. M. Yaghi, M. O'Keeffe, N. W. Ockwig, H. K. Chae, M. Eddaoudi and J. Kim, *Nature*, 2003, **423**, 705.
54. O. M. Yaghi, H. Li, C. Davis, D. Richardson and T. L. Groy, *Acc. Chem. Res.*, 1998, **31**, 474.
55. D. Britt, D. Tranchemontagne and O. M. Yaghi, *Proc. Natl. Acad. Sci.*, 2008, **105**, 11623.
56. J. L. C. Rowsell and O. M. Yaghi, *Microporous and Mesoporous Mater.*, 2004, **73**, 3.
57. Z.-M. Zhang, T. Zhang, C. Wang, Z. Lin, L.-S. Long and W. Lin, *J. Am. Chem. Soc.*, 2015, **137**, 3197.
58. Q.-L. Zhu and Q. Xu, *Chem. Soc. Rev.*, 2014, **43**, 5468.
59. C.-Y. Sun, S.-X. Liu, D.-D. Liang, K.-Z. Shao, Y.-H. Ren and Z.-M. Su, *J. Am. Chem. Soc.*, 2009, **131**, 1883.
60. F.-J. Ma, S.-X. Liu, C.-Y. Sun, D.-D. Liang, G.-J. Ren, F. Wei, Y.-G. Chen and Z.-M. Su, *J. Am. Chem. Soc.*, 2011, **133**, 4178.
61. J. Juan-Alcañiz, J. Gascon and F. Kapteijn, *J. Mater. Chem.*, 2012, **22**, 10102.
62. J. Song, Z. Luo, D. Britt, H. Furukawa, O. M. Yaghi, K. I. Hardcastle and C. L. Hill, *J. Am. Chem. Soc.*, 2011, **133**, 16839.
63. A. Dhakshinamoorthy and H. Garcia, *Chem. Soc. Rev.*, 2012, **41**, 5262.
64. L. Bromberg and T. A. Hatton, *ACS Appl. Mater. Interfaces*, 2011, **3**, 4756.
65. L. Bromberg, Y. Diau, H. Wu, S. A. Speakman and T. A. Hatton, *Chem. Mater.*, 2012, **24**, 1664.
66. N. V. Maksimchuk, K. A. Kovalenko, S. S. Arzumanov, Y. A. Chesalov, M. S. Melgunov, A. G. Stepanov, V. P. Fedin and O. A. Kholdeeva, *Inorg. Chem.*, 2010, **49**, 2920.
67. N. V. Maksimchuk, O. A. Kholdeeva, K. A. Kovalenko and V. P. Fedin, *Isr. J. Chem.*, 2011, **51**, 281.
68. A. Aijaz, A. Karkamkar, Y. J. Choi, N. Tsumori, E. Rönnebro, T. Autrey, H. Shioyama and Q. Xu, *J. Am. Chem. Soc.*, 2012, **134**, 13926.
69. L. Bromberg, Y. Klichko, E. P. Chang, S. Speakman, C. M. Straut, E. Wilusz and T. A. Hatton, *ACS Appl. Mater. Interfaces*, 2012, **4**, 4595.
70. T. Loiseau, C. Serre, C. Huguénard, G. Fink, F. Taulelle, M. Henry, T. Bataille and G. Férey, *Chem. Eur. J.*, 2004, **10**, 1373.
71. E. G. Palacios, G. Juárez-López and A. J. Monhemius, *Hydrometallurgy*, 2004, **72**, 139.
72. M. Kurihara and H. Nishihara, *Coord. Chem. Rev.*, 2002, **226**, 125.
73. R. Liang, L. Shen, F. Jing, W. Wu, N. Qin, R. Lin and L. Wu, *Appl. Catal. B: Env.*, 2014, **162**, 245.
74. K.-L. Zhang, H.-Y. Gao, N. Qiao, F. Zhou and G.-W. Diau, *Inorg. Chim. Acta*, 2008, **361**, 153.
75. Z. Han, F. Qiu, R. Eisenberg, P. L. Holland and T. D. Krauss, *Science*, 2012, **338**, 1321.
76. J. B. Hendrickson, D. J. Cram and G. S. Hammond, in *Organic Chemistry*, McGraw-Hill, New York, 1970, pp. Chapter 8.
77. K. Suzuki, F. Tang, Y. Kikukawa, K. Yamaguchi and N. Mizuno, *Angew. Chem. Int. Ed.*, 2014, **53**, 5356.
78. C. S. Ewing, G. Veser, J. J. McCarthy, J. K. Johnson and D. S. Lambrecht, *J. Phys. Chem. C*, 2015, **119**, 19934.
79. D.-D. Han, Z.-G. Liu, J.-H. Liu and X.-J. Huang, *RSC Adv.*, 2015, **5**, 38290.
80. W. Ji, W. Qi, S. Tang, H. Peng and S. Li, *Nanomaterials*, 2015, **5**, 2203.
81. I. Schrader, S. Neumann, R. Himstedt, A. Zana, J. Warneke and S. Kunz, *Chem. Commun. (Cambridge, U. K.)*, 2015, **51**, 16221.
82. C. Zhang, S. Y. Hwang and Z. Peng, *J. Mater. Chem. A*, 2014, **2**, 19778.
83. Y. V. Geletii, A. Gueletii and I. A. Weinstock, *J. Mol. Catal. A: Chem.*, 2007, **262**, 59.
84. H. Park and W. Choi, *J. Phys. Chem. B*, 2003, **107**, 3885.
85. A. Pearson, H. Jani, K. Kalantar-zadeh, S. K. Bhargava and V. Bansal, *Langmuir*, 2011, **27**, 6661.

Table of Contents



A POM can perform four functions simultaneously, a theme of potential value in construction of energy converting multicomponent assemblies.